Direct Power Control and Fault Diagnosis of Photovoltaic Grid Connected Inverter System

Wenting JIA[1,2], Xueye WEI[1], Junhong ZHANG[1], Jianguang MA[1]

[1]*School of Electronic and Information Engineering,* Beijing Jiaotong University, Beijing, 100044, China
[2]*Department of Urban Rail Transit,* Beijing Jiaotong Vocational Technical College, Beijing, 102200, China

***Abstract* — For photovoltaic power generation systems, photovoltaic power under the condition of volatile, Distribution network automation is a technique can effectively improve the efficiency of fault handling, is one of important technologies to realize circuit fault diagnosis. The technology hardware construction and operation of power grids are put forward new requirements, this paper proposes a Direct power control and fault diagnosis of photovoltaic grid connected inverter system, which is deal with distribution network automation processing efficiency evaluation approach of fault diagnosis, based on the fault and restore the proportion of electricity power loss numerical calculation, finally get a numeric value, in order to judge the fault diagnosis processing efficiency. Doubly-fed photovoltaic power station transmission light mass through a flexible HVDC power transmission system (VSCHVDC). Unloading device is installed on the dc side in this method, using "power differences" energy imbalance caused the ends of the VSCHVDC such fan group has not stable operation of net. Combined with calculation example of a pv field in Xinjiang to make simulated analysis, the simulation result proves the effectiveness of this method.**

Keywords - photovoltaic power generation; flexible high-voltage direct current; power difference; unloading; fault detection; low voltage ride through

I. INTRODUCTION

Pv power generation is regarded as one of the main directions of the development of clean energy. In recent years, pv power generation has developed rapidly. Installed capacity is getting bigger and bigger. However, the problem of "transmission bottleneck" is becoming more and more serious. For power transmission system of VSCHVDC which is regarded as a new type of power transmission system, pv generating set can transmit the pv power in large scale through power transmission system of VSCHVDC and has good voltage regulation function at the same time so as to supply power to isolated load in remote places. It can independently control the active power and reactive power and provides a certain reactive power support to the system so as to improve power quality and other advantages. Without the combination of double-fed pv power plant, the application of VSCHVDC grid-connected system to LVRT and the solution to this problem emerging, LVRT control method of double-fed pv power plant with VSCHVDC grid-connected system is put forwarded and the application is innovative. Based on fan set grid connection of double-fed VSCHVDC, the method isolates the pv power plant from power grid. Adopt the method that restrains the voltage overtension of and unbalanced consumed power of DC bus in transmission system so as not to not affect the pv generating set and continue to contribute to fault ride-through, achieving low voltage ride through. By taking advantage of Matlab/Simulink[5] simulation platform, low voltage ride through model including double-fed pv power plant is established; the effectiveness of energy consumption of the unloading resistance device is studied. Combined with the situation of pv power transmission of a pv power plant in Dabancheng of Xinjiang, simulation study is carried out and the effectiveness of the method is proved.

II. THE MATHEMATICAL MODEL OF PV GENERATOR AND THE EQUIVALENT METHOD

A. Mathematical Model of Double-Fed Photovoltaic (pv) grid

Reference direction of voltage and current of double-fed pv power generator is selected according to motor **convention**. The d axis is in the same direction as the stator voltage vector, that is $u_{gq}=0$. The per unit value form of magnetic linkage equation and transient voltage equations [4] are:

$$\begin{cases} u_w = R_s i_g + \dfrac{d\psi_g}{dt} + j\omega_w \psi_g \\ u_r = R_r i_r + \dfrac{d\psi_r}{dt} + j(\omega_w - \omega_r)\psi_r \\ \psi_r = L_r i_r + L_m i_g \\ \psi_g = L_s i_g + L_m i_r \\ L_s = L_{s\sigma} + L_m \\ L_r = L_{r\sigma} + L_m \end{cases} \quad (1)$$

Where, u_w and u_r are stator and rotor voltage space vector respectively; i_g and i_r are stator and rotor current space vector respectively; ψ_w and ψ_r are stator and rotor

flux linkage vector respectively; R_s and R_r are stator inductance and rotor inductance respectively; $L_{s\sigma}$ and $L_{r\sigma}$ stator leakage inductance and rotor leakage inductance respectively; L_s and L_r are stator inductance and rotor inductance; ω_r is rotor electric angular frequency; ω_w is electric angular frequency of pv field voltage.

B. Equivalent Method of Double-Fed Photovoltaic (pv) grid

Select a double-fed pv power generator of which equivalent method [6-7] is double-fed pv field equivalence and keeps all the Photovoltaic (pv) grids and pv speed model; mechanical torque of double-fed pv power generator is accumulated as T_{sum}; the equivalent generator is regarded as input. Calculation formula of equivalent pv power generator is:

$$\begin{cases} S_{eq}=\sum_{i=1}^{m}S_i, P_{eq}=\sum_{i=1}^{m}P_i, C_{eq}=\sum_{i=-1}^{m}C_i \\ Z_{G-eq}=\frac{Z_G}{m}, Z_{T-eq}=\frac{Z_T}{m}, T_{sum}=\sum_{i=1}^{m}T_i \end{cases} \quad (2)$$

In the formula, ***eq*** is the equivalence of double-fed pv power generator; ***m***, ***S***,***P***,***C***,***ZG*** and ***ZT*** represent the number of pv power generator,capacity size, active power,compensating capacitor, impedance of pv power generator and impedance of transformer ofgenerator terminal.

III. MATHEMATICAL MODEL AND CONTROL SYSTEM OF VSCHVDC

VSCHVDC is regarded as the core part of LVRT structure of double-fed pv power plant with grid-connected VSCHVDC; the analysis of structure and mathematical model of VSCHVDC is closely related to each parameter setting of the unloading device.

A. Mathematical Model of VSCHVDC

Structures [8] of the two voltage source converters are the same. One-end system can be analyzed.

One-line Diagram of One-Side Convertor Station of VSCHVDC is shown in Fig. 1

In case of losses neglected, then:

$$P_s = P_{dc} \quad (3)$$

Mathematical model [9] of inverter station of VSCHVDC in abc three phase stationary coordinate system is :

$$C\frac{dU_{dc}}{dt}=\begin{bmatrix} \lambda M\cdot\cos(\omega t+\delta) \\ \lambda M\cdot\cos(\omega t-120°+\delta) \\ \lambda M\cdot\cos(\omega t+120°+\delta) \end{bmatrix}\begin{bmatrix} i_a \\ i_b \\ i_c \end{bmatrix}-i_{dc.line} \quad (4)$$

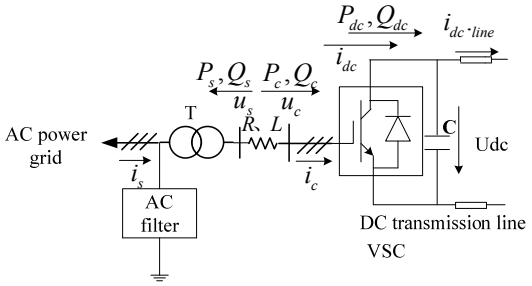

Figure 1. One-line diagram of one-side convertor station of VSCHVDC

The formula (4) can be transformed to the dq synchronous rotating coordinate system [7]; it can be obtained:

$$C\frac{dU_{dc}}{dt}=\frac{3\lambda M}{2}(i_d\cos\delta+i_q\sin\delta)-i_{dc.line} \quad (5)$$

Where, λ is the fixed value and is related to PWM modulation [10] model; δ is the included angle between output voltage of VSC AC side and AC voltage of the system; M is modulation ratio; the subscript dc is the DC side parameter.

B. Control System of VSCHVDC

VSC at both ends of VSCHVDC control system can control active power separately; the premise is to keep the active power balanced at both ends as great changes in active power directly influence the change in the DC side voltage[11]. Therefore, influence between rectifier side and inverter side is showed in the change in active power.

The control charts are shown in Fig. 2 and Fig.3 respectively.

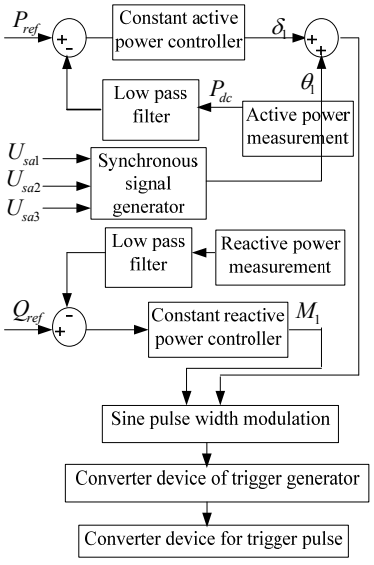

Figure 2. Control chart of connecting rectifier side of VSCHVDC transmission system

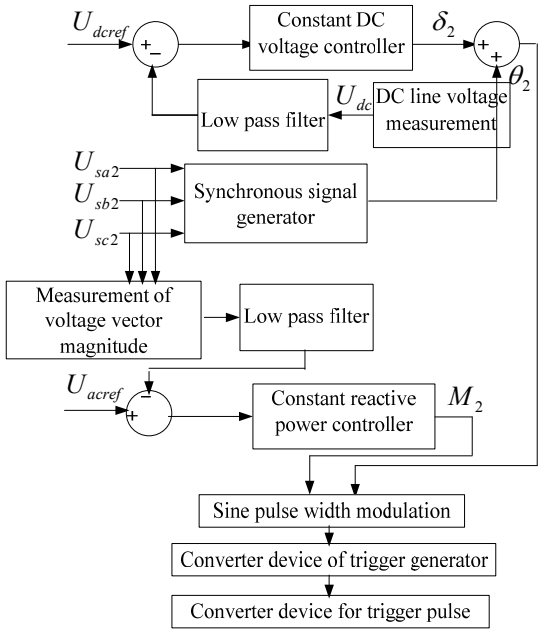

Figure 3. Control block chart of connecting inverter side of transmission system

Parameter controlled by active power of rectifier side is δ_1; parameter controlled by reactive power of rectifier side is M1; parameter controlled by AC voltage is M2.

IV. RESEARCH ON THE FAULT RIDE-THROUGH METHOD BASED ON VSCHVDC GRID CONNECTION

New high voltage DC transmission is grid connected with pv power plant; when pv power is output, the probability of failure at the output of the grid connected system is the highest. Specific to the voltage drop of fault point after AC power grid fault,the research on low voltage ride through control of double-fed pv power plant through VSCHVDC grid connection is mainly to eliminate surplus power energy of VSCHVDC DC side so as to keep transmission power balanced.

As VSCHVDC grid connected transmission system is new high voltage direct current transmission, active power consumption of transmission lines is relatively less [12-13] and can be ignored. When the AC system has failure which causes power imbalance, assumed that power difference is ΔP,

$$\Delta P = \left| \frac{3}{2} u_{sd} i_d - u_{dc} i_{dc} \right| = u_{dc} C \frac{du_{dc}}{dt} \qquad (6)$$

From formula (6), when power is unbalanced, namely $\Delta P \neq 0$, the change rate of DC voltage is not zero. Therefore, DC voltage fluctuation of VSCHVDC can be regarded as a symbol of imbalanced power of the system.

By adopting DC unloading resistance and through connecting fully-controlled type electronic valve in DC line of power grid side, the control circuit is shown in Fig. 4:

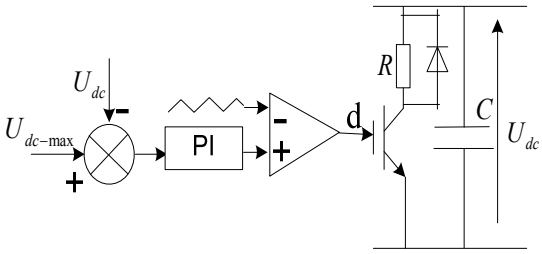

Figure 4. Fault Ride through control circuit based on unloading resistance

When the system is in normal operation, protection circuit does not work. When a fault occurs on the AC side of the power grid which causes the voltage drops; input power of the DC side is bigger than changes in output power and the DC side voltage, at this time the unloading device is triggered to consume the excess energy and at the same time restrain the voltage of the DC side so as to protect the transmission system.

As unloading device mainly consumes the surplus power of the DC side, the symbol of direct control is the voltage variation of the DC side; trigger pulse circuit is controlled according to voltage variation of the DC side. Logic Control Block Diagram of Unloading Device is shown in Fig.5:

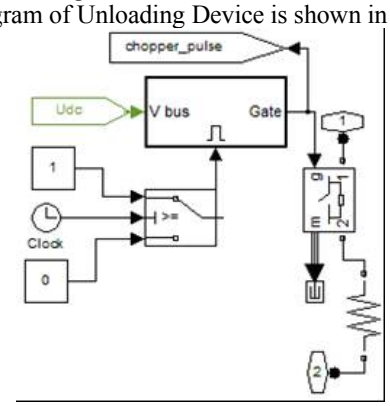

(a) Logic control chart of unloading part

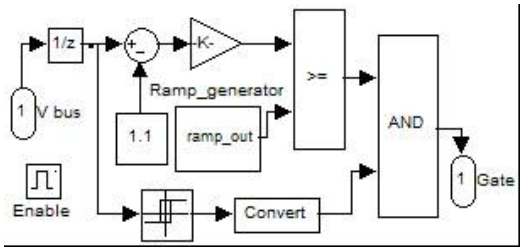

(b) Logic control chart of the DC side voltage and trigger signal

Figure 5. Logic control block diagram of unloading device

The selection of unloading resistance size is mainly related to the allowable maximum voltage of the DC side and the required consumption of maximum power [14].

$$R = \frac{U_{dc-\max}^2}{\Delta P_{\max}} \tag{7}$$

Where, $U_{dc-\max}$ is the allowable voltage upper limit of DC bus; $\Delta P_{\max}$ is the maximum power [15-16] consumed. The duty cycle of circuit input is:

$$d = \frac{C_{dc}(U_{dc} - U_{dc-\max})}{U_{dc-\max} R} \tag{8}$$

$$\begin{cases} U_{dc} > U_{dc-\max}, \text{Triggering} \\ U_{\mathrm{dc}} \le U_{dc-\max}, \text{No triggering} \end{cases} \tag{9}$$

LVRT control of VSCHVDC grid connected system of double-fed pv power plant focuses on detecting the change in the DC side voltage; when the DC side voltage is more than the allowed maximum value, the unloading device will be immediately input; when the DC side voltage is less than the allowed maximum value, the unloading device will be removed.

V. APPLICATION CALCULATION EXAMPLE SIMULATION AND SIMULATION ANALYSIS

LVRT control of VSCHVDC double-fed pv power plant is put forwarded and is mainly used for transmission delivery and long distance transmission of pv power in remote places.

In order to prove LVRT control of VSCHVDC grid connected system of double-fed pv power plant and the effectiveness of consuming excess energy of unloading device loaded at the DC side, based on MATLAB/Simulink, the simulation model of VSCHVDC and double-fed pv power plant grid-connected low voltage ride-through device is established.

The calculation example is that a double-fed pv power plant in Dabancheng of Xinjiang is accessed to an infinite power system and VSCHVDC transmission system. Refer to actual operating parameters of a demonstration project in Denmark and is shown in Fig. 6.

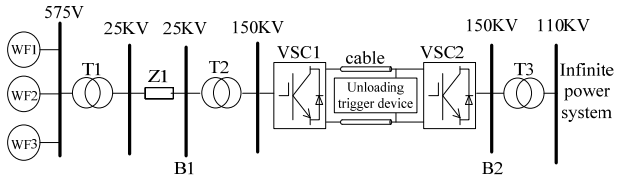

Figure 6. Diagram of calculation example structure

Mainly including: pv power plant consists of three sub equivalent pv fields; three equivalent pv fields are the same; each sub pv field consists of 20 double-fed pv power generators with 1.5MW and 10 double-fed pv power generators with 1MW. Equivalent parameters are shown in Table 1

Table 1. Parameters of equivalent photovoltaic (pv) grid

Parameter	Single parameter		Parameter of equivalent Photovoltaic (pv) grids
	20	10	
	20	10	
Rated power (MW)	1.5	1	40
Rated voltage (V)	575	575	575
Frequency (Hz)	50	50	50
Inertia constant (s)	5.04	3.5	4.116
Damping coefficient (pu)	0.01	0.01	0.01
Stator resistance (PU)	0.00706	0.00488	0.0206
Stator reactance (PU)	0.171	0.1386	0.1982
Rotor resistance (PU)	0.005	0.00549	0.0053
Rotor reactance (PU)	0.156	0.1493	0.1520
Excitation reactance (PU)	2.9	3.9527	3.5015
Initial slip frequency	0.2	0.2	0.2

Outlet voltage of pv field is 575V and is changed to 25KV through T1 transformer; then transmitted to B1 after 1km; changed to 150KV through T2 transformer; the cable length of The DC side is 180km and is changed to 110KV through the transformer at the place of B2 so as to be accessed to an infinite power system.

The system fault is set at B2; the failure time is at 0.6s; the fault continues for 625ms; the fault is removed at 1.225s;the pv speed is set to constant speed of 15m/s, various parameter waveforms will appear in Fig.7 and Fig.8.

A. Analysis of System Fault Voltage

From simulation result of Fig.7, when the fault is at 0.6s of Fig. (a), output voltage at B2 of outlet end drops, dropping to 20% of the rated voltage and output voltage recovers at 1.225s when the fault is removed. From Fig. (b), when the fault occurs, DC voltage begans to rise; trigger pulse is not set to "1"; when the DC side voltage rises to the allowable voltage limit of DC bus, the trigger pulse is set to "1" immediately. From Fig. (c), output voltage of double-fed pv power plant is kept constant which shows that the fan set does not operate out of grid with constant output during a fault.

From three waveforms of Fig.7, after the fault occurs at fault point, the whole system is in stable operation and the volatility is not big; trigger device is ready to enter or leave according to changes in voltage of the DC side. From simulation result, the simulation results are in agreement with the theoretical analysis which shows that the voltage index meets the requirements of national grid low voltage ride through.

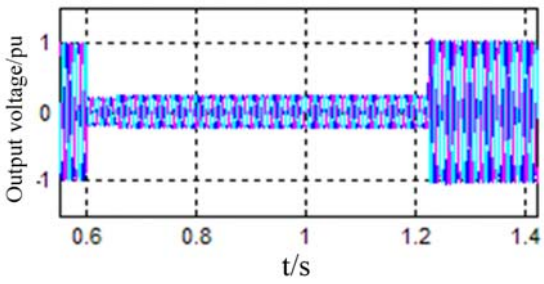

(a) Output voltage waveform

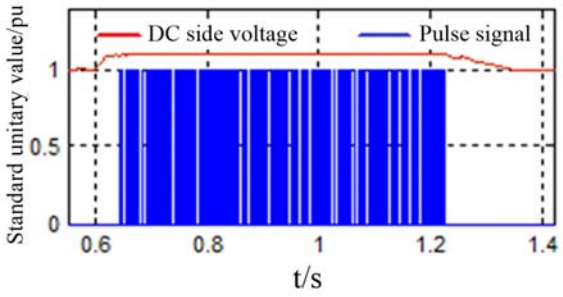

(b) Waveforms of DC voltage and trigger pulse

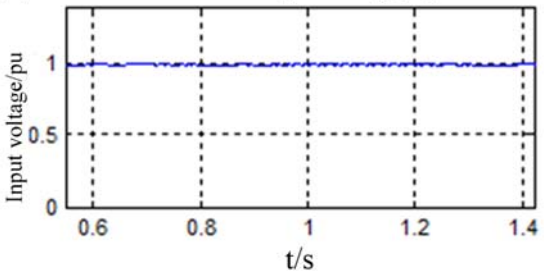

(c) Input Voltage Waveform

Figure 7. Output voltage, the DC side voltage,trigger pulse and input voltage

B. Analysis of System Fault Power

It can be seen from the simulation results of Fig. 8: in Fig (a), after the fault occurs, since the system is large and complex, in the input and output moment of the fault, the system is affected by some fluctuations, but the output voltage basically stays the same; the output power is reduced during the fault, and the unloading resistance is put into operation. In Fig. (b), the difference of the output power before and after the fault is about 38MW, which will lead to the increase of the difference between the input and the output power; this part of power difference is transferred into HVDC transmission line, which has about 38MW power accumulation. It can be seen from the simulation Fig. (c) that during the fault period, due to the unavoidable line loss of the transmission system, the power of the unloading resistance is approximately equal to the declined power of the output terminal. The unloading resistance effectively dissipates the accumulation power on the HVDC side, and protects the transmission system and the operation equipment.

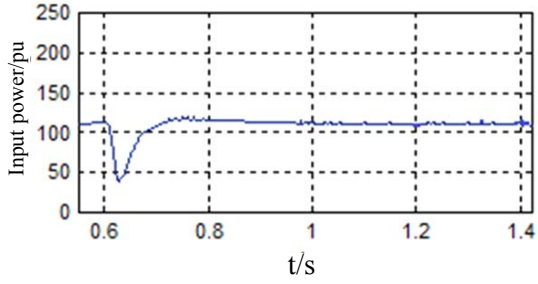

(a) Input power waveform

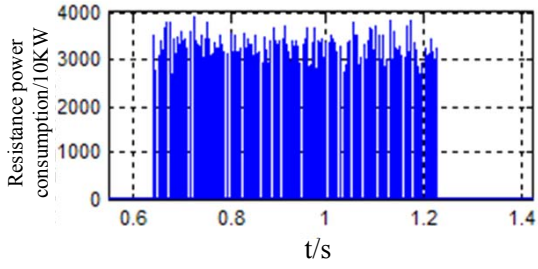

(b) Power waveform of the unloading part

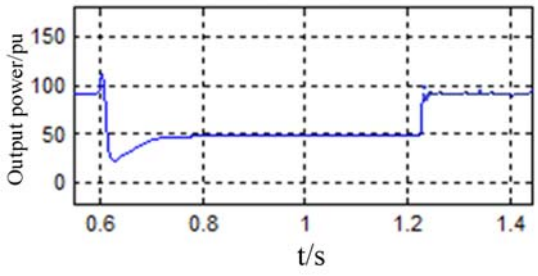

(c) Output power waveform

Figure 8. Input power, unloading resistance power and output power

From the whole analysis of Fig. 7 and Fig. 8, it can be seen that: in the Fig. 7 (b) and Fig. 8 (b), the trigger pulse and unloading part are in synchronization. At the happening and ending of the fault, the slightly impact appears in the system , which is within the allowed scope of the system. When the fault 625ms is over, the system recovers to the former state, which shows that this method can meet the requirement of low voltage ride-through.

VI. CONCLUSIONS

LVRT control method of VSCHVDC grid connected system of double-fed pv power plant is analyzed. In Matlab/Simulink, low voltage ride-through model including double-fed pv power plant is established. Combined with simulation examples, System power device switching frequency is fixed, is advantageous for the output filter design; The introduction of negative vector effect time correction mechanism, solves the dynamic power response caused by too much power in the process of mutation slow problem, which can effectively broaden the photovoltaic (pv) grid inverter system applied in the complex environment, load and changeable in the distributed generation system.

REFERENCES

[1] Ouchen S, Betka A, Abdeddaim S, et al. Fuzzy-predictive direct power control implementation of a grid connected photovoltaic system, associated with an active power filter[J]. Energy Conversion & Management, 2016, 122:515-525.

[2] Chen Y, Shen F, Hu R. Control Technology of 10kW Photovoltaic Grid-Connected Inverter Based on TMS320F2808[J]. Applied Mechanics & Materials, 2015, 734:893-896.

[3] Kumar N, Saha T K, Dey J. Modeling, control and analysis of cascaded inverter based grid-connected photovoltaic system[J]. International Journal of Electrical Power & Energy Systems, 2016, 78:165-173.

[4] Rajeev M, Agarwal V. Closed loop control of novel transformer-less inverter topology for single phase grid connected photovoltaic system[C]// IEEE Power and Energy Conference at Illinois. IEEE, 2016.

[5] Raj M M P. Cascaded H-Bridge Five-Level Inverter for Grid-Connected Photovoltaic System Using Proportional-Integral Controller[J]. Measurement and Control -London- Institute of Measurement and Control-, 2016, 49(1):33-41.

[6] N.F. Guerrero-Rodríguez, Alexis B. Rey-Boué, Luis C. Herrero-de Lucas, et al. Control and synchronization algorithms for a grid-connected photovoltaic system under harmonic distortions, frequency variations and unbalances[J]. Open Renewable Energy Journal, 2015, 80:380-395.

[7] Bouhafs A, Lokmane B M, Mohamed D. Grid Connected Photovoltaic System, for a 800 W ☆ [J]. Energy Procedia, 2015, 74:414-422.

[8] Menadi A, Abdeddaim S, Ghamri A, et al. Implementation of fuzzy-sliding mode based control of a grid connected photovoltaic system[J]. Isa Transactions, 2015, 58:586-594.

[9] Jinyu Hu, Zhiwei Gao and Weisen Pan. Multiangle Social Network Recommendation Algorithms and Similarity Network Evaluation[J]. Journal of Applied Mathematics, 2013 (2013).

[10] Guanxiong Liu, Yishuang Geng, Kaveh Pahlavan, Effects of calibration RFID tags on performance of inertial navigation in indoor environment, 2015 International Conference on Computing, Networking and Communications (ICNC), Feb. (2015).

[11] Jie He, Yishuang Geng, Yadong Wan, Shen Li, Kaveh Pahlavan, A cyber physical test-bed for virtualization of RF access environment for body sensor network, IEEE Sensor Journal, 13(10), 3826-3836, Oct. (2013).

[12] Shuang Zhou, Liang Mi, Hao Chen, Yishuang Geng, Building detection in Digital surface model, 2013 IEEE International Conference on Imaging Systems and Techniques (IST), Oct. (2012).

[13] Jie He, Yishuang Geng, Kaveh Pahlavan, Toward Accurate Human Tracking: Modeling Time-of-Arrival for Wireless Wearable Sensors in Multipath Environment, IEEE Sensor Journal, 14(11), 3996-4006, Nov. (2014).

[14] Lv Z, Halawani A, Fen S. Touch-less Interactive Augmented Reality Game on Vision Based Wearable Device[J]. Personal and Ubiquitous Computing, (2015), 19(3): 551-567.

[15] Guanqun Bao, Liang Mi, Yishuang Geng, Mingda Zhou, Kaveh Pahlavan, A video-based speed estimation technique for localizing the wireless capsule endoscope inside gastrointestinal tract, 2014 36th Annual International Conference of the IEEE Engineering in Medicine and Biology Society (EMBC), Aug. (2014).

[16] Degui Zeng, Yishuang Geng, Content distribution mechanism in mobile P2P network, Journal of Networks, 9(5), 1229-1236, Jan. (2014).

.